

Article

The Jet-Disk Coupling of Seyfert Galaxies from a Complete Hard X-ray Sample

Xiang Liu ^{1,2,*}, Ning Chang ^{1,3}, Zhenhua Han ⁴ and Xin Wang ^{1,3}

¹ Xinjiang Astronomical Observatory, Chinese Academy of Sciences, 150 Science 1-Street, Urumqi 830011, China; changning@xao.ac.cn (N.C.); wangxin2019@xao.ac.cn (X.W.)

² Physics and Astronomy Department, Qiannan Normal University for Nationalities, Duyun 558000, China

³ School of Astronomy and Space Science, University of Chinese Academy of Sciences, Beijing 100049, China;

⁴ Physics and Electronic Engineering Department, Xinjiang Normal University, Urumqi 830000, China; hanzhh@xjnu.edu.cn

* Correspondence: liux@xao.ac.cn

Received: 28 March 2020; Accepted: 7 May 2020; Published: 10 May 2020



Abstract: We analyze the jet-disk coupling for different subsamples from a complete hard X-ray Seyfert sample to study the coupling indices and their relation to accretion rate. The results are: (1) the power-law coupling index ranges from nearly unity (linear correlation) for radio loud Seyferts to significantly less than unity for radio quiet ones. This decline trend of coupling index also holds from larger sources to compact ones; (2) the Seyferts with intermediate to high accretion rate (Eddington ratio $\lambda \sim 0.001$ to 0.3) show a linear jet-disk coupling, but it shallows from near to super Eddington ($\lambda \sim 0.3$ to 10), and the former is more radio loud than the latter; (3) the Seyfert 1s are slightly steeper than the Seyfert 2s, in the jet-disk correlation. In the linear coupling regime, the ratio of jet efficiency to radiative efficiency (η/ϵ) is nearly invariant, but in low accretion or super accretion regime, η/ϵ varies with λ in our model. We note that a radio-active cycle of accretion-dominated active galactic nuclei would be: from a weaker jet-disk coupling in $\lambda < 0.001$ for low luminosity Seyferts, to a linear coupling in $0.001 < \lambda < 0.3$ for radio-loud luminous Seyferts and powerful radio galaxies/quasars, and to a weaker coupling in $0.3 < \lambda < 10$ ones.

Keywords: Seyfert galaxies; accretion rate; jet power; jet-disk coupling

1. Introduction

Active galactic nuclei (AGNs) are the most powerful sources in the Universe and believed to be powered by their central massive black hole accretion. In the meantime, there are significant feedbacks from AGN to host galaxy. The accretion and feedback together have formed the co-evolution of the AGN and its host galaxy. In addition to the AGN winds and slow outflows to host galaxy, radio jet (collimated outflow) is a prominent feedback from AGN to host galaxy and to intergalactic medium, although the jetted phase of AGN is only about 10% of its whole life from large AGN sample statistics [1]. Thus, a big question is why AGN is radio silence (non-jetted) in most of its lifetime, but active in its whole lifetime in optical and probably in X-rays. Most AGNs are identified in optical field from local Seyfert galaxies to distant quasars.

For the complexity of AGN structure, their electromagnetic emissions are believed to be multi-components. The optical continuum (including UV and part of IR) and hard X-rays are thought to be mainly from the accretion disk and its corona. The bolometric disk luminosity is often scaled proportionally to the optical emission or hard X-rays from the disk, which is regulated by the mass accretion rate (or Eddington ratio) [2,3]. It is possible that an AGN evolves from low to high accretion rate, then reversely from high to low rate, for a lifetime (or episode) cycle of AGN. A jetted phase is

present only in a part time ($\sim 10\%$) of a life cycle of AGN, it is not clear which part of the accretion cycle (accretion rates) the jetted phase is most correlated.

We know that the accretion disk luminosity is proportional to the mass accretion rate in the form of $L_{\text{disk}} = \epsilon \dot{M} c^2$, with ϵ the disk radiative efficiency, c the speed of light. A jet power can be

$$P_j = 1.3 \times 10^{38} (\eta/\epsilon) [(L_{\text{disk}}/L_{\text{Edd}})M] (\text{erg s}^{-1}) \propto (\eta/\epsilon) L_{\text{disk}}, \quad (1)$$

where η is the jet efficiency depending on jet production mechanism, the Eddington ratio $\lambda = L_{\text{disk}}/L_{\text{Edd}}$, with L_{Edd} the Eddington luminosity, M the black hole (BH) mass in solar mass unit.

We can see that the jet-disk coupling is relative to the η/ϵ in Equation (1), which may be otherwise not constancy for different type of sources which being at different accretion rates [4]. We absorb this unknown factor η/ϵ in Equation (1) into the power-law index μ in the form of

$$P_j = c_1 \times (\eta/\epsilon) L_{\text{disk}} = c_2 \times L_{\text{disk}}^\mu = c_3 \times L_{\text{disk}}^{1+q} \propto (\lambda M)^{1+q}, \quad (2)$$

assuming η/ϵ is also a function of the disk luminosity as $\eta/\epsilon = \text{function}(L_{\text{disk}}) = \text{const} \times L_{\text{disk}}^q$, thus $\mu = 1 + q$, where c_1 , c_2 , and c_3 are constants. With this model, we can fit the relation of jet power and disk luminosity with μ and derive the q , in order to study the jet-disk coupling for different subsamples. These subsamples should come from a well-defined complete sample. In the literature, there are discussions of the impact of magnetic flux [5] and the black hole spin [6,7] on the jet-disk correlation, which may introduce some scatter in the correlation.

In this paper, we reanalyze the complete hard-X-ray Seyfert sample by Panessa et al. [8] in more detail, in order to investigate the jet-disk coupling for different subsamples. In the Panessa sample, the 2–10 keV X-ray flux is from Malizia et al. [9], the radio data mainly come from the NRAO (National Radio Astronomy Observatory) VLA (Very Large Array) Sky Survey (NVSS; Condon et al. [10]) at 1.4 GHz, with additional complements being from the Sydney University Molonglo Sky Survey (SUMSS; Bock et al. [11]) at 843 MHz, see Section 3 for more details. In order to avoid strong Doppler boosting effect (thus the luminosities measured are far away from their intrinsic values), sources like blazars are not included in this sample.

2. Some Previous Statistics and Models

There are several statistical findings that radio power almost linearly correlates with the emission line luminosity or accretion disk luminosity in powerful radio galaxies and quasars [12–15]. These results are often explained by the accretion-jet model [14,16]. On the other hand, the statistical results of low luminosity AGNs (LLAGNs) show shallower correlations of jet-disk coupling [17–19] with the power-law indices of 0.4–0.7 as summarized in [20]. This relative weak jet-disk coupling in the LLAGNs may be attributed either to an inefficient accretion [21] or to the BH spin-jet model [20,22–24].

There are also statistical results showing rather steeper (with power-law index of ~ 1.4) radio-X-ray correlation for AGN [25] and for BH X-ray binaries' outliers-track [4,26], which are possibly regulated by radiatively efficient accretion flow or disk-corona model [27–29].

Panessa et al. [8] presented a complete hard X-ray sample of relatively luminous Seyfert galaxies, and found significant correlation with slopes being consistent with those expected for radiatively efficient accreting systems. This complete sample consists of a couple of subsamples, which were not analyzed individually in [8].

3. The Subsample Analysis on Jet-Disk Coupling

The Panessa et al. sample [8] is a well-defined complete hard X-ray sample of relatively high luminosity AGN at $z < 0.36$, including Seyfert 1s and Seyfert 2s, with X-ray (2–10 keV and 20–100 keV) and radio data from NVSS at 1.4 GHz (or for some sources, the 843 MHz has been converted into 1.4 GHz flux density assuming a spectral index of -0.7 , $S \propto \nu^{-0.7}$). The radio morphologies are classified as

resolved (R), slightly resolved (S), and unresolved (U) (whose size smaller than one-half the restoring beam size at full width at half-maximum (FWHM = 45 arcsec), e.g., for a source at redshift of ~ 0.1 typical in our study, the unresolved size is ≤ 23 kpc) and the rms noise in the images are about 0.5–1 mJy/beam. Black hole mass is available for most of the sources. Therefore, we can estimate the radio jet power, bolometric disk luminosity ($20L_X$ (2–10 keV), [8]), Eddington ratio, and X-ray radio loudness ($R_X = L_R/L_X$ (2–10 keV), with $\text{Log} R_X > -4.5$ for radio loud and $\text{Log} R_X < -4.5$ for radio quiet, as defined in [30]). The mechanical radio jet power P_j (rather than radio luminosity $L_{1.4}$ by [8]) is used for including the work on environment by jet, expressed as $P_j \sim 2.05 \times 10^7 (L_{1.4})^{6/7}$ (erg s^{-1}) [15,20], and the integrated flux density of source is adopted. The error of jet power is very small (not shown) in the log-log plot, considering an error of radio flux density of $<10\%$ for the VLA data. Here, we assume that the model of jet power [15] which derived mainly from massive BHs in FRI and FRII sources, can be used to the relatively lower BH masses of Seyfert galaxies in our sample.

From a total of 71 Seyfert galaxies with radio detections, we define two subgroups with 41 Seyfert 1s (including Seyfert 1 to Seyfert 1.5), and 30 Seyfert 2s (including Seyfert 1.9 to Seyfert 2) according to [8]. The BH mass in the two samples are comparable with the average of $10^{7.7}$, $10^{7.4}$, and median value of $10^{7.5}$, $10^{7.6}$ solar mass, for Seyfert 1s and 2s, respectively. The X-ray luminosity L_X (2–10 keV) distributes roughly flat versus Eddington ratio as shown in Figure 1a for the Seyfert 1s and 2s. The radio jet power (at 1.4 GHz) is positively correlated with the radio loudness, and ranges similarly for the Seyfert 1s and 2s in Figure 1b.

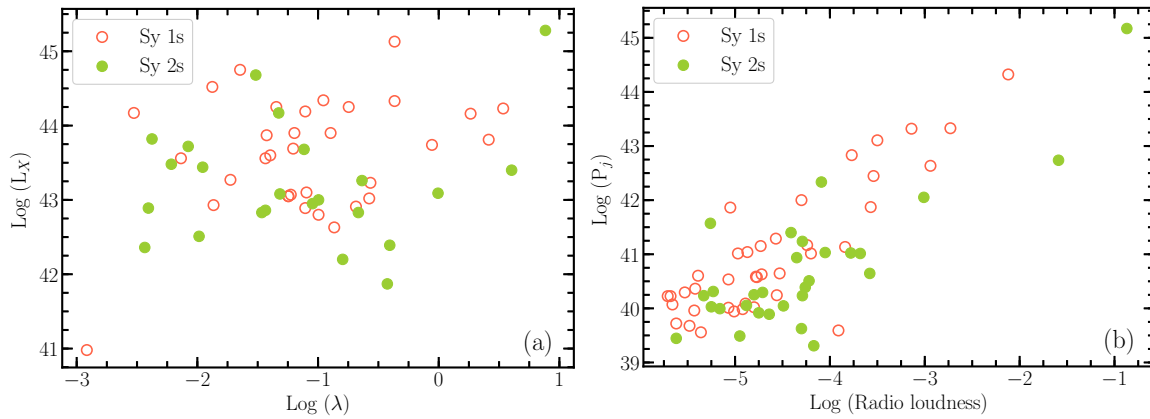


Figure 1. (a) Log (X-ray luminosity in 2–10 keV) vs. Log (Eddington ratio λ) for Seyfert 1s (red) and 2s (green). (b) Log (jet power in erg s^{-1}) vs. Log (radio loudness) for Seyfert 1s (red) and 2s (green).

The coupling index between radio jet power and disk luminosity is shown in Figure 2a, for Seyfert 1s and 2s, with the steep index of 1.12 ± 0.18 in Seyfert 1s and 0.84 ± 0.21 in Seyfert 2s.

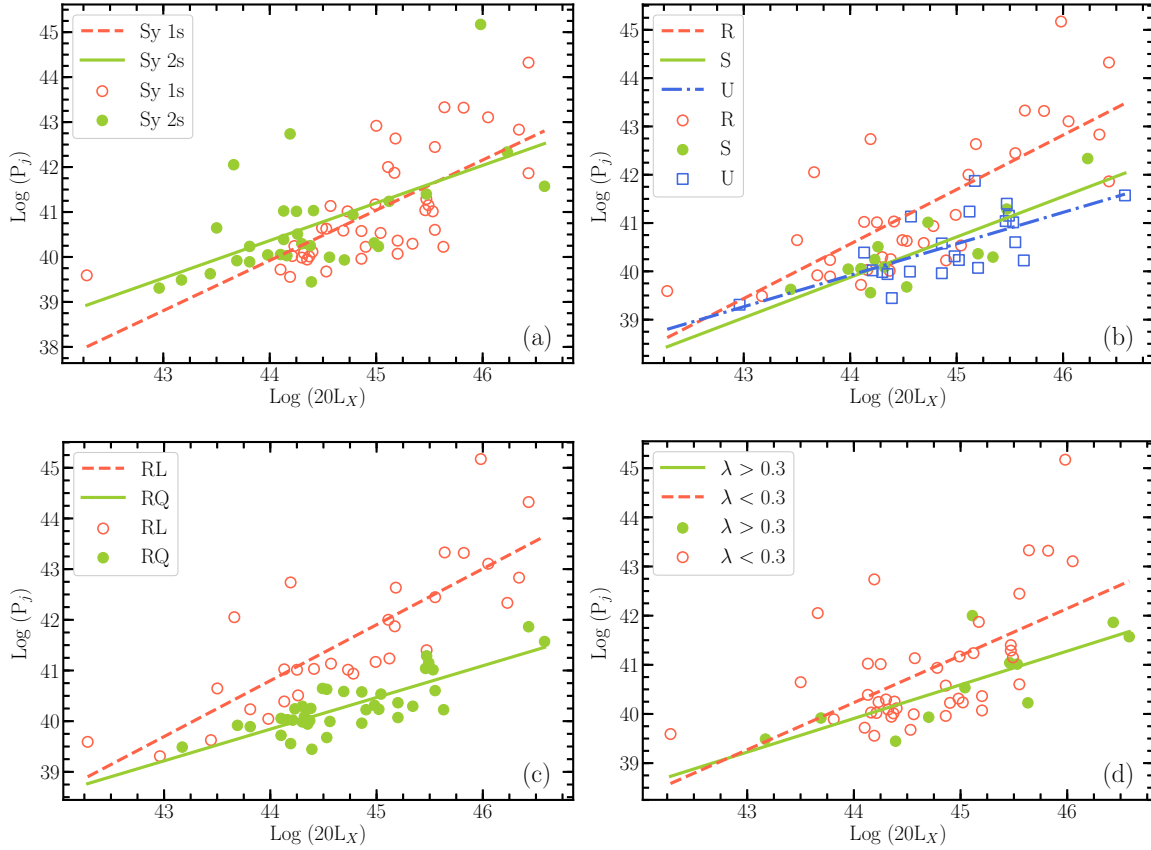


Figure 2. (a) Log (jet power in erg s^{-1}) vs. Log (disk luminosity in erg s^{-1}), with the best linear fit $y = (1.12 \pm 0.18)x - 9.22$, and $y = (0.84 \pm 0.21)x + 3.58$, for Seyfert 1s (red) and Seyfert 2s (green). (b) Log (jet power) vs. Log (disk luminosity), with the best linear fit $y = (1.13 \pm 0.17)x - 9.06$, $y = (0.84 \pm 0.18)x + 3.08$, and $y = (0.65 \pm 0.15)x + 11.27$ for resolved (red), slightly resolved (green), and unresolved radio sources (blue), respectively. (c) Log (jet power) vs. Log (disk luminosity), with the best linear fit $y = (1.10 \pm 0.15)x - 7.76$, and $y = (0.63 \pm 0.08)x + 12.32$ for radio loud (red) and radio quiet sources (green). (d) Log (jet power) vs. Log (disk luminosity), with the best linear fit $y = (0.68 \pm 0.18)x + 9.77$, and $y = (0.96 \pm 0.21)x - 1.89$ for sources with Eddington ratio $\lambda > 0.3$ (green) and those with $\lambda < 0.3$ (red).

The fitted slopes are 1.13 ± 0.17 , 0.84 ± 0.18 , and 0.65 ± 0.15 for the resolved, slightly resolved, and unresolved sources, respectively in Figure 2b.

The slopes for radio loud and radio quiet Seyferts are shown in Figure 2c with a nearly linear correlation (1.10 ± 0.15) for radio loud and a shallower correlation (0.63 ± 0.08) for radio quiet ones.

The slope of the subsample in near to super accretion rate (Eddington ratio $0.3 < \lambda < 10$) and that in moderate to high accretion rate ($0.001 < \lambda < 0.3$) is 0.68 ± 0.18 and 0.96 ± 0.21 , respectively in Figure 2d. It is surprising that the jet-disk coupling index is lower at the very high accretion rates.

The slopes for larger BHs ($>10^{7.6}$ suns) and smaller BHs ($<10^{7.6}$ suns) are 0.75 ± 0.34 and 0.47 ± 0.17 , respectively, with a large error of slope or a low significance of correlation in Table 1.

Table 1. The results of linear regression fits and correlation coefficients for $\text{Log } P_j = \mu \text{Log}(20L_X) + b$, the columns are (1) subsample (Seyfert 1s, Seyfert 2s, resolved source by VLA, S: slightly resolved by VLA, U: unresolved by VLA, radio loud, radio quiet, Eddington ratio > 0.3 , Eddington ratio < 0.3 , BH mass $M_{\text{BH}} > 10^{7.6} M_\odot$, BH mass $M_{\text{BH}} < 10^{7.6} M_\odot$, respectively); (2) sample size; (3) median value of $\text{Log } P_j$ and $\text{Log}(20L_X)$; (4) power-law slope μ in $P_j = c_1 \times (\eta/\epsilon) L_{\text{disk}} = c_2 \times L_{\text{disk}}^\mu = c_3 \times L_{\text{disk}}^{1+q}$, assuming $\eta/\epsilon = \text{const} \times L_{\text{disk}}^q$, where $P_j \sim 2.05 \times 10^7 (L_{1.4})^{6/7} \text{ (erg s}^{-1}\text{)}$ and $L_{\text{disk}} = 20L_X \text{ (2–10 keV) (erg s}^{-1}\text{)}$; (5)–(7) Pearson, Spearman, and Kendall correlation coefficient (and probability for rejecting the null hypothesis that there is no correlation), (8) $q = \mu - 1$.

Subsample (1)	Size (2)	Median($P_j, 20L_X$) (3)	μ (4)	Pearson(p_{null}) (5)	Spearman(p_{null}) (6)	Kendall(p_{null}) (7)	q (8)
Seyfert 1	41	(40.6, 45.0)	1.12 ± 0.18	0.70 (2.9×10^{-7})	0.75 (1.5×10^{-8})	0.56 (3.6×10^{-7})	0.12 ± 0.18
Seyfert 2	30	(40.3, 44.3)	0.84 ± 0.21	0.59 (5.5×10^{-4})	0.53 (2.9×10^{-3})	0.40 (2.1×10^{-3})	-0.16 ± 0.21
Resolved	33	(40.9, 44.5)	1.13 ± 0.17	0.76 (2.4×10^{-7})	0.73 (1.5×10^{-6})	0.55 (6.5×10^{-6})	0.13 ± 0.17
S	13	(40.2, 44.3)	0.84 ± 0.18	0.82 (6.4×10^{-4})	0.79 (1.5×10^{-3})	0.62 (2.7×10^{-3})	-0.16 ± 0.18
U	22	(40.4, 45.0)	0.65 ± 0.15	0.69 (3.5×10^{-4})	0.65 (1.1×10^{-3})	0.43 (4.8×10^{-3})	-0.35 ± 0.15
R_{loud}	30	(41.2, 44.8)	1.10 ± 0.15	0.82 (3.4×10^{-8})	0.84 (5.8×10^{-9})	0.69 (9.5×10^{-8})	0.10 ± 0.15
R_{quiet}	38	(40.2, 44.6)	0.63 ± 0.08	0.81 (7.7×10^{-10})	0.73 (2.1×10^{-7})	0.53 (3.7×10^{-6})	-0.37 ± 0.07
$\lambda > 0.3$	11	(40.5, 45.1)	0.68 ± 0.18	0.78 (4.8×10^{-3})	0.76 (7.3×10^{-3})	0.56 (0.016)	-0.32 ± 0.18
$\lambda < 0.3$	42	(40.4, 44.6)	0.96 ± 0.21	0.58 (5.5×10^{-5})	0.54 (2.0×10^{-4})	0.41 (1.4×10^{-4})	-0.04 ± 0.21
$M_{\text{BH}} > 10^{7.6}$	29	(41.2, 45.2)	0.75 ± 0.34	0.42 (0.025)	0.47 (9.7×10^{-3})	0.34 (9.1×10^{-3})	-0.25 ± 0.34
$M_{\text{BH}} < 10^{7.6}$	24	(40.0, 44.3)	0.47 ± 0.17	0.52 (9.2×10^{-3})	0.35 (0.091)	0.22 (0.14)	-0.53 ± 0.17

The radio loudness versus the disk luminosity shows a bi-model alike distribution, the radio loud ones (RLs) show slightly positive correlation, and the radio quiet ones (RQs) show a slightly negative correlation in Figure 3a. These positive and negative correlations (with the power-law index of ρ) can be explained with the steeper index $\mu = 1.1$ of jet-disk coupling in the RLs and the shallower $\mu = 0.63$ in the RQs (Figure 2c), for $P_j \propto L_{1.4}^{6/7}$ and $P_j \propto (L_{\text{disk}})^\mu = (20L_X)^\mu$:

$$R_{\text{loudness}} = L_{1.4}/L_X \propto L_X^{(7/6)\mu-1} = L_X^\rho \propto L_{\text{disk}}^\rho, \quad (3)$$

where $\rho = (7/6)\mu - 1$.

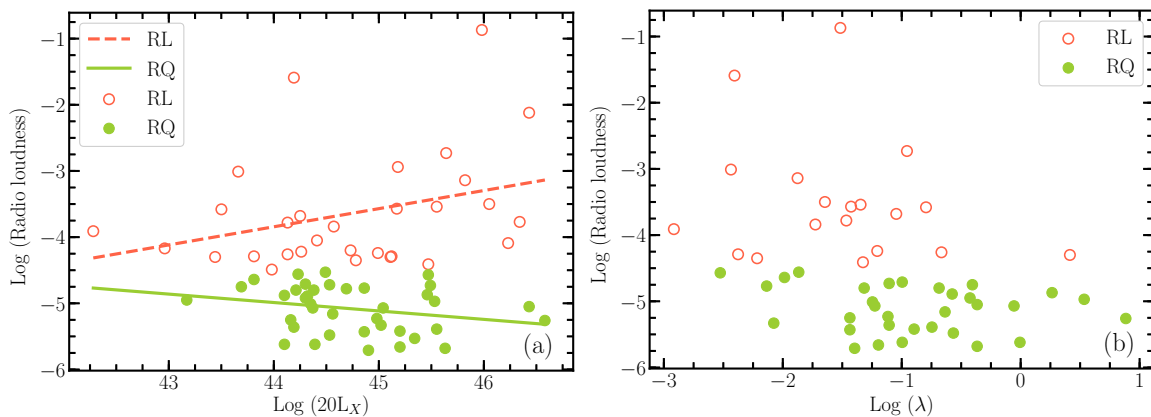


Figure 3. (a) Log (radio loudness) vs. Log (disk luminosity in erg s^{-1}), with the best linear fit $y = (0.27 \pm 0.15)x - 15.89$, and $y = (-0.13 \pm 0.08)x + 0.61$, for radio loud (red) and radio quiet sources (green). (b) Log (radio loudness) vs. Log (Eddington ratio) for radio loud (red) and radio quiet sources (green).

For the whole sample, the radio loudness shows a decrease trend from Eddington ratio of 0.001 to 0.3 (or -3 to -0.5 in log scale), and has no significant correlation with the accretion rate in $0.3 < \lambda < 10$, in Figure 3b. Implications of the Figure 3b are discussed in Section 4.

The results for the slope of jet-disk coupling, correlation coefficient (with probability) of the subsamples are summarized in Table 1. We will discuss the results further as following.

4. Discussion

We use the $20L_X$ (2–10 keV) as approximate bolometric disk luminosity. The higher energy luminosity in 20–100 keV (L_{HX} in short) is also available in the Panessa et al. sample [8], who plotted the radio luminosity $L_{1.4}$ versus either L_X (2–10 keV) or L_{HX} (20–100 keV), showing that the radio-X-ray correlation slope is steeper in L_{HX} band than in L_X band. This is caused by the non-linear correlation of $L_{HX} \propto L_X^{0.84 \pm 0.04}$ as we fitted. The L_X (2–10 keV) is widely used to estimate the bolometric disk luminosity (e.g., [8,17,31]), and the high energy loss (or break) in the 20–100 keV band would prevent the L_{HX} as a good estimate for bolometric disk luminosity.

The hard X-ray selected sample is almost unbiased with respect to absorption compared with the optical estimate for bolometric disk luminosity, and the Seyferts are mostly located in the nearby Universe, reducing as much as possible the selection (e.g., distance) effects [9]. The Seyfert 1s, 2s, and R, S, U sources are equally distributed in redshift [8], and K-corrections are ignored in our analysis since the redshifts for our Seyferts are relatively small (≤ 0.36), and the correlation results in Table 1 should be not caused by the redshift or distance effects [32].

We obtained various jet-disk coupling indices (from 0.47 to 1.13) for different subsamples from the complete hard X-ray Seyfert sample. The linear correlation of jet-disk coupling ($\mu \sim 1$), e.g., in the radio loud Seyferts, leads to $q = \mu - 1 = 0$, i.e., a constant ratio of $\eta/\epsilon \propto L_{\text{disk}}^{q=0} = \text{constant}$. This implies both the jet efficiency η and disk radiative efficiency ϵ are invariant, or they vary proportionally in the radio loud Seyferts. The linear correlation can be explained in Equation (2) with the invariant ratio η/ϵ , and which is often referred to the accretion-dominated jet, as also shown in FRII quasars [14] and thought to be regulated by radiatively efficient accretion flow or disk corona model [25,28,29].

The Seyfert 1s are usually more face-on to us than the Seyfert 2s, however, the beaming effect may not cause a steeper index of jet-disk coupling but can cause the scatter of the coupling as analyzed in [33]. There are slightly larger median values of P_j and $20L_X$ in the Seyfert 1s than in Seyfert 2s (see column 3 in Table 1), implying probably a potential contribution of L_X from the jet base in Seyfert 1s. This effect would be not significant as noted in [32].

The index of jet-disk coupling, e.g., in the radio quiet sources (but not radio silence), is shallower, with $\mu < 1$, $q = \mu - 1 < 0$, i.e., $\eta/\epsilon \propto L_{\text{disk}}^{q<0} \propto (\lambda M)^{q<0}$. This implies the ratio of jet efficiency η and disk radiative efficiency ϵ varies with disk luminosity (or accretion rate and BH mass) for the radio quiet sources.

There is a decline trend of radio loudness vs. Eddington ratio λ from 0.001 to 0.3, and no significant correlation with λ from 0.3 to 10 in Figure 3b in the Seyfert galaxies. The decline part in the intermediate to high accretion regime shows a linear jet-disk coupling in Figure 2d, whereas in the near to super Eddington regime there is a shallower index ($\mu = 0.68 \pm 0.18$) in Figure 2d with a low significance of correlation in Table 1. The result implies that very high accretion (near to super Eddington) may quench the jet, as noted in [34]. There are similar decline trends between radio loudness and accretion rates as also found in [2,5,35].

Furthermore, we used $20L_X$ (2–10 keV) as an approximation of the bolometric disk luminosity, we note that in Vasudevan and Fabian [36], the bolometric disk luminosity is about $20L_X$ (2–10 keV) in Eddington ratio less than 0.2, but has a sharp increase to $\sim 60L_X$ (2–10 keV) in $\lambda > 0.2$. We have tried to test the jet-disk correlations by using the two bolometric corrections of disk luminosity in the two accretion regimes respectively, the correlation results in Table 1 are almost not changed. A future study should consider the bolometric correction dependence on accretion rate with a well-fitted function.

On the other hand, the low luminosity AGNs (Eddington ratio around $\lambda \sim 0.0001$ or less) show smaller indices (0.4–0.7) of jet-disk coupling [20], that could be explained by radiatively inefficient accretion flows (RIAF, [21]) and/or by the BH spin-powered jet (because of the spin-jet power being weakly correlated with the accretion rate, [20,23]).

In addition, we propose that a radio-active cycle of accretion-dominated AGN would be: from a weak jet-disk coupling ($\mu < 1, q < 0$) in low Eddington ratio ($\lambda < 0.001$) in cosmic LLAGNs (excluding local radio-loud LLAGNs which we called ‘pseudo’ radio-loud ones in the sense of a distant universe), to a linear (or even steeper) correlation ($\mu \geq 1, q \geq 0$) in intermediate to high Eddington ratio ($0.001 < \lambda < 0.3$) for radio-loud luminous Seyferts and powerful radio galaxies/quasars [14], and to a weak coupling ($\mu < 1, q < 0$) again in near to super Eddington ($0.3 < \lambda < 10$) (with a quenched/frustrated jet and a weak dependence of the ratio η/ε on accretion rate).

In this scenario, the most of accretion-dominated AGNs may live in their radio loud phase ($\sim 10\%$ of AGN lifetime) in the middle regime of accretion rate with an efficient (linear or steeper) jet-disk coupling, especially for luminous Seyfert galaxies in this paper and for FR II quasars in [14]. In this idea we do not consider local LLAGNs that are about 50% radio loud [18,19], for that the fraction will be much smaller for a distant universe due to radio undetectability of the local LLAGNs) and their jet might not be accretion dominated but BH-spin dominated [20].

Moreover, another fundamental factor seems to be changes in the spectral energy distribution (SED), which is driven by changes in the type of accretion disk (RIAF, standard disk, superluminous disk) for different regimes of accretion rates [2,37], that may partly be related to the function of ratio η/ε on accretion rate and BH mass, and so the coupling of mechanical (jet) vs. radiative (disk) power, e.g., in Equation (2).

5. Summary and Conclusions

We reanalyzed the jet-disk coupling for various subsamples of a complete hard X-ray Seyfert sample in order to study the coupling indices and their relation to accretion rate. The results are: (i) the power-law coupling index ranges from nearly unity (linear correlation) for radio loud Seyferts to significantly less than unity for radio quiet ones. This decline trend of coupling index also holds from larger sources to compact ones; (ii) the Seyferts with intermediate to high accretion rate (Eddington ratio $\lambda \sim 0.001$ to 0.3) show a linear jet-disk correlation, and the coupling shallows from near to super Eddington ($\lambda \sim 0.3$ to 10), and the former is more radio loud than the latter; (iii) the Seyfert 1s have a slightly steeper jet-disk coupling than the Seyfert 2s.

A theoretical implication of the results is that, in the linear coupling regime, the ratio of jet efficiency to radiative efficiency (η/ε) is nearly invariant, whereas in the low accretion or super accretion regime, η/ε varies with λ in our model of Equation (2).

A radio-active cycle of accretion AGN would be: from a weak jet-disk coupling in low Eddington ratio ($\lambda < 0.001$) for LLAGNs, to a linear correlation in intermediate to high Eddington ratio ($0.001 < \lambda < 0.3$) for radio-loud luminous Seyferts and powerful radio galaxies/quasars, and to a weak coupling again in near to super Eddington ($0.3 < \lambda < 10$). In this scenario, the most of accretion-dominated AGNs may live as a radio loud source in the middle regime of accretion rate with an efficient (linear) jet-disk coupling, especially for radio-loud luminous Seyferts and quasars.

Author Contributions: Conceptualization, writing—original draft, X.L.; plotting and editing, N.C.; and review and editing, Z.H. and X.W. All authors have read and agreed to the published version of the manuscript.

Funding: This work is supported by the National Key R&D Program of China under grant number 2018YFA0404602, and the Key Laboratory of Radio Astronomy, Chinese Academy of Sciences.

Acknowledgments: We thank Luis C. Ho and Fu-Guo Xie for usefull comments on the manuscript.

Conflicts of Interest: The authors declare no conflict of interest.

References

1. Condon, J.J.; Kellermann, K.I.; Kimball, A.E.; Ivezić, Ž.; Perley, R.A. Active Galactic Nucleus and Starburst Radio Emission from Optically Selected Quasi-stellar Objects. *Astrophys. J.* **2013**, *768*, 37.
2. Ho, L.C. Nuclear activity in nearby galaxies. *Annu. Rev. Astron. Astrophys.* **2008**, *46*, 475–539.
3. Netzer, H. Bolometric correction factors for active galactic nuclei. *Mon. Not. R. Astron. Soc.* **2019**, *488*, 5185–5191.
4. Xie, F.-G.; Yuan, F. Interpreting the radio/X-ray correlation of black hole X-ray binaries based on the accretion-jet model. *Mon. Not. R. Astron. Soc.* **2016**, *456*, 4377–4383.
5. Sikora, M.; Stawarz, L.; Lasota, J.-P. Radio Loudness of Active Galactic Nuclei: Observational Facts and Theoretical Implications. *Astrophys. J.* **2007**, *658*, 815–828.
6. Miller, J.M.; Reynolds, C.S.; Fabian, A.C.; Miniutti, G.; Gallo, L.C. Stellar-Mass Black Hole Spin Constraints from Disk Reflection and Continuum Modeling. *Astrophys. J.* **2009**, *697*, 900–912.
7. Unal, C.; Loeb, A. On Spin Dependence of the Fundamental Plane of Black Hole Activity. *arXiv* **2020**, arXiv:2002.11778.
8. Panessa, F.; Tarchi, A.; Castangia, P.; Maiorano, E.; Bassani, L.; Bicknell, G.; Bazzano, A.; Bird, A.J.; Malizia, A.; Ubertini, P. The 1.4-GHz radio properties of hard X-ray-selected AGN. *Mon. Not. R. Astron. Soc.* **2015**, *447*, 1289–1298.
9. Malizia, A.; Stephen, J.B.; Bassani, L.; Bird, A.J.; Panessa, F.; Ubertini, P. The fraction of Compton-thick sources in an INTEGRAL complete AGN sample. *Mon. Not. R. Astron. Soc.* **2009**, *399*, 944–951.
10. Condon, J.J.; Contton, W.D.; Greisen, E.W.; Yin, Q.F.; Perley, R.A.; Taylor, G.B.; Broderick, J.J. The NRAO VLA Sky Survey. *Astron. J.* **1998**, *115*, 1693–1716.
11. Bock, D.C.; Large, M.I.; Sadler, E.M. SUMSS: A Wide-Field Radio Imaging Survey of the Southern Sky. I. Science Goals, Survey Design, and Instrumentation. *Astron. J.* **1999**, *117*, 1578–1593.
12. Cao, X.; Rawlings, S. No evidence for a different accretion mode for all 3CR FR I radio galaxies. *Mon. Not. R. Astron. Soc.* **2004**, *349*, 1419–1427.
13. Rawlings, S.; Saunders, R. Evidence for a common central-engine mechanism in all extragalactic radio sources. *Nature* **1991**, *349*, 138–140.
14. van Velzen, S.; Falcke, H. The contribution of spin to jet-disk coupling in black holes. *Astron. Astrophys.* **2013**, *557*, L7.
15. Willott, C.J.; Rawlings, S.; Blundell, K.M.; Lacy, M. The emission line-radio correlation for radio sources using the 7C Redshift Survey. *Mon. Not. R. Astron. Soc.* **1999**, *309*, 1017–1033.
16. Blandford, R.D.; Payne, D.G. Hydromagnetic flows from accretion disks and the production of radio jets. *Mon. Not. R. Astron. Soc.* **1982**, *199*, 833–903.
17. Ho, L.C. Radiatively Inefficient Accretion in Nearby Galaxies. *Astrophys. J.* **2009**, *699*, 626–637.
18. Ho L.C.; Peng C.Y. Nuclear Luminosities and Radio Loudness of Seyfert Nuclei. *Astrophys. J.* **2001**, *555*, 650–662.
19. Nagar, N.M.; Falcke, H.; Wilson, A.S. Radio sources in low-luminosity active galactic nuclei. IV. Radio luminosity function, importance of jet power, and radio properties of the complete Palomar sample. *Astron. Astrophys.* **2005**, *435*, 521–543.
20. Su, R.Z.; Liu, X.; Zhang, Z. Correlation analysis of radio properties and accretion-disk luminosity for low luminosity AGNs. *Astrophys. Space Sci.* **2017**, *362*, 3.
21. Yuan F.; Narayan R. Hot Accretion Flows Around Black Holes. *Annu. Rev. Astron. Astrophys.* **2014**, *52*, 529–588.
22. Blandford, R.D.; Znajek, R.L. Electromagnetic extraction of energy from Kerr black holes. *Mon. Not. R. Astron. Soc.* **1977**, *179*, 433–456.
23. Liu, X.; Han, Z.H.; Zhang, Z. The physical fundamental plane of black hole activity: Revisited. *Astrophys. Space Sci.* **2016**, *361*, 9.
24. Tchekhovskoy, A.; Narayan, R.; McKinney, J.C. Efficient generation of jets from magnetically arrested accretion on a rapidly spinning black hole. *Mon. Not. R. Astron. Soc.* **2011**, *418*, L79–L83.
25. Dong A.-J.; Wu Q.-W.; Cao X.-F. A New Fundamental Plane for Radiatively Efficient Black-hole Sources. *Astrophys. J.* **2014**, *787*, L20.

26. Gallo, E.; Miller, B.; Fender, R. Assessing luminosity correlations via cluster analysis: evidence for dual tracks in the radio/X-ray domain of black hole X-ray binaries. *Mon. Not. R. Astron. Soc.* **2012**, *423*, 590–599.
27. Falcke, H.; Körding, E.; Markoff, S. A scheme to unify low-power accreting black holes. Jet-dominated accretion flows and the radio/X-ray correlation. *Astron. Astrophys.* **2004**, *414*, 895–903.
28. Heinz, S.; Sunyaev, R.A. The non-linear dependence of flux on black hole mass and accretion rate in core-dominated jets. *Mon. Not. R. Astron. Soc.* **2003**, *343*, L59–L64.
29. Qiao, E.; Liu, B.F. A disc corona-jet model for the radio/X-ray correlation in black hole X-ray binaries. *Mon. Not. R. Astron. Soc.* **2015**, *448*, 1099–1106.
30. Terashima, Y.; Wilson, A.S. Chandra Snapshot Observations of Low-Luminosity Active Galactic Nuclei with a Compact Radio Source. *Astrophys. J.* **2003**, *583*, 145–158.
31. Merloni, A.; Heinz, S.; Di Matteo, T. A Fundamental Plane of black hole activity. *Mon. Not. R. Astron. Soc.* **2003**, *345*, 1057–1076.
32. Gupta, M.; Sikora, M.; Rusinek, K. Comparison of SEDs of very massive radio-loud and radio-quiet AGN. *Mon. Not. R. Astron. Soc.* **2020**, *492*, 315–325.
33. Heinz, S.; Merloni, A. Constraints on relativistic beaming from estimators of the unbeamed flux. *Mon. Not. R. Astron. Soc.* **2004**, *355*, L1–L5.
34. Greene, J.E.; Ho, L.C.; Ulvestad, J.S. The Radio Quiescence of Active Galaxies with High Accretion Rates. *Astrophys. J.* **2006**, *636*, 56–62.
35. Ho, L.C. On the Relationship between Radio Emission and Black Hole Mass in Galactic Nuclei. *Astrophys. J.* **2002**, *564*, 120–132.
36. Vasudevan, R.V.; Fabian, A.C. Piecing together the X-ray background: bolometric corrections for active galactic nuclei. *Mon. Not. R. Astron. J.* **2007**, *381*, 1235–1251.
37. Xie F.-G.; Zdziarski A.A. Radiative Properties of Magnetically Arrested Disks. *Astrophys. J.* **2019**, *887*, 167.



© 2020 by the authors. Licensee MDPI, Basel, Switzerland. This article is an open access article distributed under the terms and conditions of the Creative Commons Attribution (CC BY) license (<http://creativecommons.org/licenses/by/4.0/>).